02

分置

RB2 Pre-test Calculation using PAPAS-2S based on a Preliminary Post-test Calculation of the RB1 Test

June, 1998

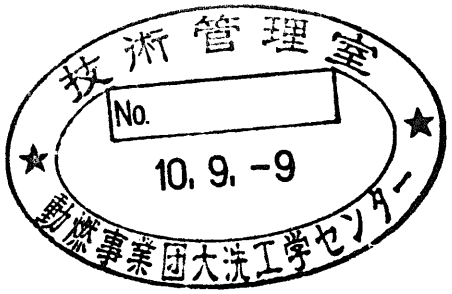

OARAI ENGINEERING CENTER
POWER REACTOR AND NUCLEAR FUEL DEVELOPMENT CORPORATION

動力炉・核燃料開発事業団（Power Reactor and Nuclear Fuel Development Corporation）

PNC TN9410 98-058
June, 1998

RB2 Pre-test Calculation using PAPAS-2S based on a Preliminary Post-test Calculation of the RB1 Test

Yoshitaka FUKANO* Ikken SATO*

Abstract

Based on the RB1 test result in the CABRI-RAFT Program, it was agreed between the partners to perform the RB2 test which aims at observation of molten fuel ejection into the coolant channel at further fuel melting and at confirmation of coolability of ejected fuel.

In this study, a preliminary post-test calculation for the RB1 test is performed first to reflect the fuel thermal condition expected for the pins with the special artificial defect preparation. Pre-test calculations for the RB2 test are then performed based on the results of this RB1 calculation. Power and coolant flow histories as well as the axial location of defect were selected as parameters in this study and a set of test condition is proposed which is believed to be most suitable to fulfill the test objectives.

*Fast Reactor Safety Engineering Section, Safety Engineering Division, O-arai Engineering Center, PNC

PNC TN9410 98-058
1998年6月

PAPAS-2Sコードによる RB1 予備的試験解析に基づく RB2 試験事前解析

深野　義隆＊　佐藤　一憲＊

要旨

CABRI-RAFT 計画の RB1 試験結果に基づき、より進んだ燃料溶融での冷却材中への溶融燃料放出挙動の観察及び放出燃料の冷却性を確認する RB2 試験を実施することがパートナー間で合意された。

本研究では、特別な人工欠陥を施したピンの燃料熱条件を反映した RB1 試験の予備的試験解析をまず実施し、この RB1 試験の解析に基いて RB2 試験の事前解析を実施した。

この事前解析では、出力及び冷却材の流量履歴、人工欠陥の軸方向位置をパラメータとし、試験目的を充足する最適な試験条件を提案した。

＊大洗工学センター　安全工学部　高速炉安全工学室

Contents

List of Tables

List of Figures

1. Introduction

In the CABRI-RAFT program, the first transient test RB1[1],[2],[3] was performed, where slow TOP was applied to an artificially pre-defected fuel pin. In this test, a fuel areal melt fraction of ~20% was reached at the cladding defect location. However, molten fuel was kept inside the pin without ejection into the coolant channel. This test result demonstrated a favorable safety characteristic of the FBR fuel under a partial fuel melting condition. Based on this result, it was agreed between the CABRI partners to perform the RB2 test which aims at observation of molten fuel ejection into the coolant channel at higher fuel melting.

In this study, a preliminary post-test calculation for the RB1 test was performed as the first step to reflect the fuel thermal condition of the Scarabix pin with the special defect preparation[4]. Then, RB2 pre-test calculation was performed with parametrically varying power histories, times of LOF initiation and axial locations of defect.

Through this study, an RB2 test condition is proposed, which is believed to be most suitable to fulfill the test objectives.

2. Preliminary post-test calculation for the RB1 test

2-1. Analytical condition

The PAPAS-2S code was used in this study. The input data for RB1 used here were prepared from those used for the MF2 test[5] in which the Scarabix fuel was used as well. Starting from the MF2 data, necessary modifications to reflect the RB1 test condition were given such as: steady-state linear power rating, axial power profile, coolant flowrate, coolant temperature at BFC (bottom of fissile column), transient power and coolant flowrate histories. With these modifications, TFC (top of fissile column) coolant temperature at the steady state and transient was reasonably simulated for the RB1 test.

It was expected through preliminary calculations that the fuel thermal condition consistent with MF2 would result in underestimation of fuel melting especially around the midplane. Therefore, three cases given in Table 1 with different fuel thermal conductivity and fuel-cladding gap conductance were introduced in order to simulate the real characteristic of the RB1 fuel.

2-2. Analytical results and discussion

Figures 1 and 2 show coolant temperature at the TFC in the experiment and analysis. The analytical result gives reasonable agreement with the experimental result. Figure 3 shows the fuel melting boundary at scram for each analytical case. In the RB1-base case, where fuel thermal conductivity is decreased down to 60 % of

the nominal value to simulate development of grain boundary separation, fuel melting is overestimated compared with the RB1 test data. It is expected that fuel thermal conductivity and/or gap conductance of the real RB1 test fuel are much higher than those adopted in the RB1-base case. Therefore, it is assumed that reduction of fuel thermal conductivity is not effective for the RB1 fuel. In addition, the fuel-cladding gap conductance at a closed gap condition is assumed to be higher than the nominal value of 0.8W/cm2/K, i.e., 1.0W/cm2/K and 1.3W/cm2/K for the cases RB1-Hg10 and RB1-Hg13, respectively. In the RB1-Hg10 case, fuel melting region at ~47 cmBFC (cm above BFC) seems to be consistent with the experimental observation. However, this case overestimates fuel melting at the midplane (~38 cmBFC). On the other hand, the RB1-Hg13 case with the higher fuel-cladding gap conductance gives reasonable fuel melting at the midplane while underestimates fuel melting at ~47 cmBFC.

Although it is not clear whether higher fuel thermal conductivity or gap conductance is responsible for the real RB1 situation, these cases can simulate the global thermal characteristic of the RB1 fuel reasonably well.

3. Pre-test calculation for the RB2 test

3-1. Analytical condition

The assumption for fuel thermal conductivity and gap conductance used in the RB1-Hg10 case was used here as the reference because of the reason discussed later in this section.

Six cases given in Table 2 with different power and coolant flow histories as well as different defect locations were performed. The ramp rate and the coolant temperature at the BFC are the same as those of the RB1 test. It is also assumed in this study that the brazing temperature just before LOF initiation in the RB1 test is sufficient to prevent an early defect failure. In accordance with this assumption, the nominal coolant flowrate for each case is selected so that the defect temperature (at assumed axial location and at cladding midwall) just before LOF initiation is equal to the RB1 condition.

If the defect is placed at a higher location, more margin can be provided to avoid coolant boiling by keeping the necessary high brazing temperature after the LOF. This higher margin can give higher cladding temperature at the defect part and thereby provide more potential to open the slit circumferentially. On the other hand, too high axial location may lead to too small fuel melting. Furthermore, there is a spacer grid slightly above the midplane which may affect post-failure behavior. Thus the location of ~47 cmBFC is considered to be an only reasonable candidate which can avoid the spacer location. It is necessary, therefore, to check whether fuel melting at ~47 cmBFC is sufficient to fulfill the RB2 test objectives.

In this respect, assumption of the RB1-Hg10 case which will give reasonable overall thermal characteristics of the RB1 fuel with possible slight overestimation of fuel melting at the midplane is considered to be appropriate for the RB2 test evaluation.

Depending on assumed defect locations, an initial coolant flowrate is selected so that the same brazing temperature before LOF can be obtained. Concerning the power history, two power plateau conditions at 1000W/cm and 1100W/cm and a continued ramp condition up to 1248W/cm like the MF2 test are adopted. In the analytical cases with power plateau, LOF is initiated at the arrival to the plateau. On the other hand, in the cases with continued ramp, the LOF initiations at 1000W/cm and 1100W/cm are adopted.

3-2 . Analytical result and discussion

Figure 4 shows calculated fuel melting boundaries just before the LOF onset for the 1000PPN, 1100PPN and the 1000UPPER cases. At the arrival to 1000W/cm in all cases, fuel melting is only slightly larger than the RB1 result. This slight difference of coolant flowrate between the 1000PPN and 1000UPPER cases does not give large difference in the fuel melting. On the other hand, at the arrival to 1100W/cm, fuel melting is much more pronounced compared with the RB1 result. Therefore, if the LOF is initiated at 1100W/cm and fuel ejection takes place, this fuel melting may be beyond the threshold for fuel ejection. In this case, information of the threshold for fuel ejection will be lost. It seems more attractive, therefore, to give brazing failure at 1000W/cm and increase fuel melting in a case of no meaningful ejection.

Figure 5 shows the coolant temperature histories at the TFC for the 1000PPN and the 1000UPPER cases. The calculated coolant temperature of the 1000UPPER case shows a large margin against coolant boiling that may inhibit precise observation of molten fuel ejection. In a case of no fuel ejection after the LOF, one can realize further fuel melting with continued power increase as simulated in the 1248PPN and 1248UPPER cases. Figure 6 shows the coolant temperature histories at TFC for these two cases. Coolant boiling occurs before reaching 1150 W/cm in the 1248PPN case. In contrast to this, there is no coolant boiling in the 1248UPPER case. Furthermore, cladding temperature at the defect location reaches as high as 815 deg C, which is higher than the RB1 test condition where coolant boiling took place.

Figure 7 shows calculated final fuel melting boundaries for the 1248UPPER and 1000UPPER cases. In the 1248UPPER case, the areal melt fraction at the defect location exceeds 60%, demonstrating the advantage of the continued power ramp condition combined with the defect location at ~47 cmBFC. In any analytical cases, no meaningful difference of fuel melting between the midplane and ~47 cmBFC is observed.

Therefore, the condition used in the 1248UPPER case is considered to be the most appropriate and will provide advantages, such as high margin to coolant boiling and high potential to realize circumferential slit opening.

4. Conclusion

Through the preliminary RB1 post-test calculation, special treatment to be consistent with the observed fuel melting was introduced. With this treatment, various RB2 test conditions were parametrically checked. Through this study, the following test conditions are proposed as the most promising one.

- defect location: 47 cm from the BFC
- power history: continued power ramp up to CABRI driver limit
- coolant temperature at the BFC: 246 ℃ (same as RB1)
- initial coolant flowrate: 184.7 g/s
- linear power rating to initiate the LOF: 1000 W/cm
- LOF characteristic: normalized flowrate history same as that of RB1

If one needs a more margin to avoid coolant boiling at the final state, the initial flowrate can be slightly increased as far as the brazing temperature after LOF is sufficiently high.

Reference

[1] Ch. Marquie, et al., "Quick Look Report of the CABRI RB1 Test," CABRI NOTE C1209/97, July 1997.

[2] J.C. Giacalone, "Resultats Experimentaux Des Examens Non Destructifs Realatifs a L'essai RB1," NOTE TECHNIQUE 50/97, Nov. 1997.

[3] Ch. Marquie, et al., "Analysis Report for the CABRI RB1 Test," CABRI NOTE C1217/98, Apr. 1998.

[4] C. Gonnier, et al., "RB1 Feasibility Studies: Status on June 1996," CABRI NOTE C1183/96, June 1996.

[5] M. C. Anselmet, et al., "Analysis Report of the MF2 Experiment," CABRI NOTE C1192/96, Nov. 1996.

Table 1 Analytical cases for the RB1 post-test calculation

Case Name	Reduction of fuel thermal conductivity with grain boundary separation (% nominal value)	maximum fuel-cladding gap conductance ($W/cm^2/℃$)
RB1-base	40	0.8
RB1-Hg10	0	1.0
RB1-Hg13	0	1.3

Table 2 Analytical cases for the RB2 pre-test calculation

Case Name	slit location [cm from the BFC] (inlet flow rate [g/s])	power increase after the LOF	maximum fuel-cladding gap conductance ($W/cm^2/℃$)
1000PPN	37.5 (145.9)	NO	1.0
1100PPN	37.5 (170.1)	NO	1.0
1000UPPER	47.0 (184.7)	NO	1.0
1248PPN	37.5 (145.9)	YES	1.0
1248UPPER	47.0 (184.7)	YES	1.0

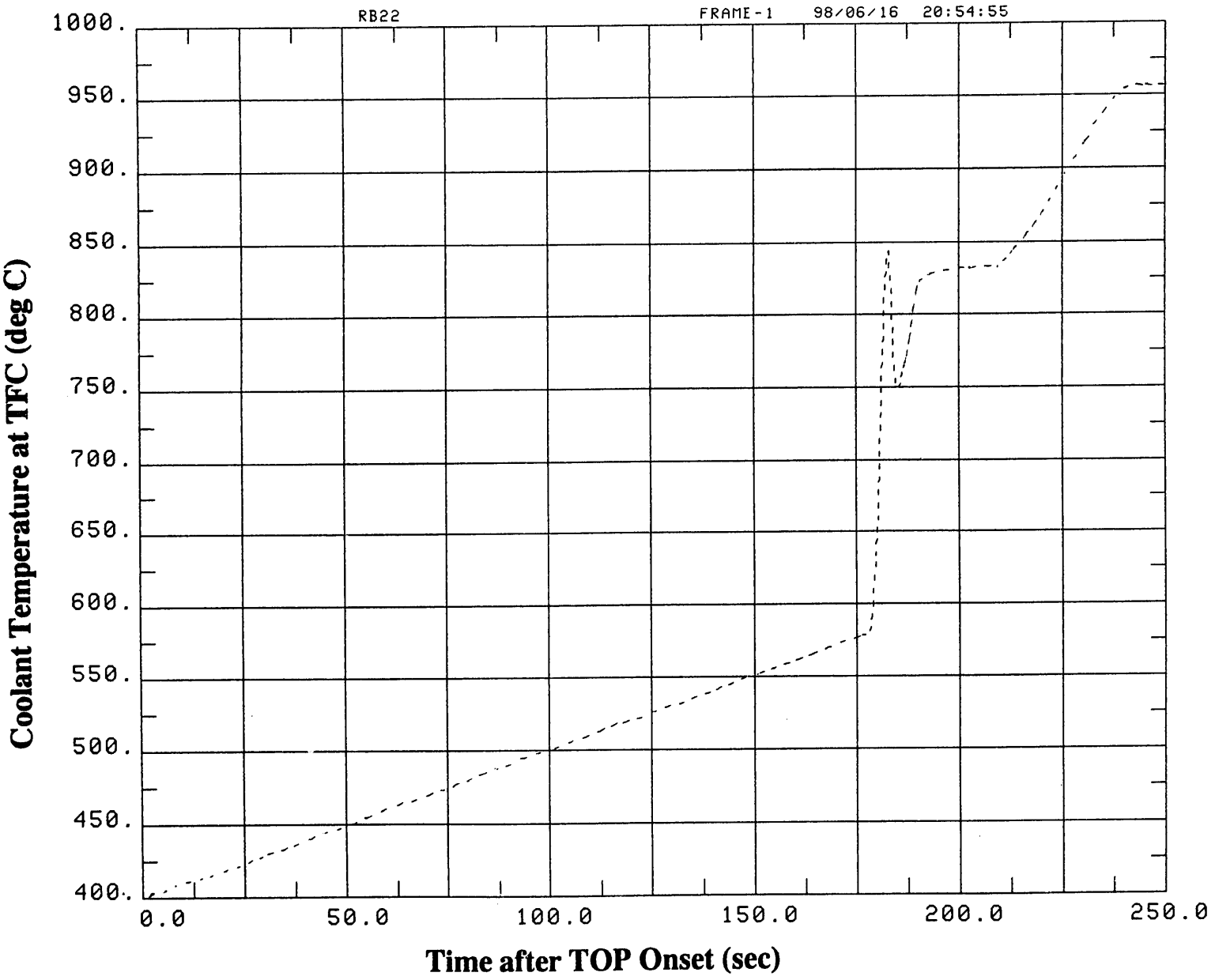

Fig. 1 Coolant temperature at the TFC in the analysis

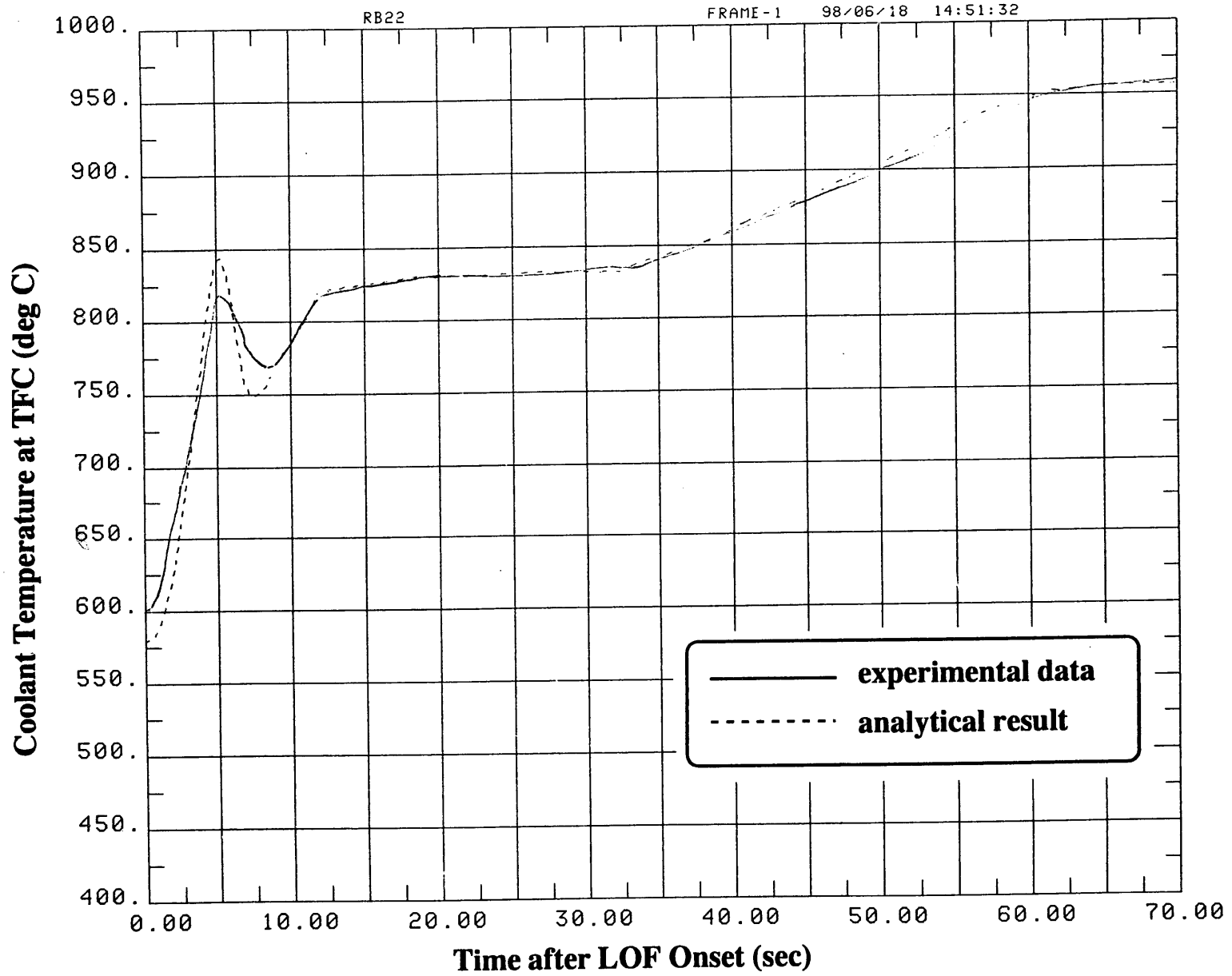

Fig. 2 Coolant temperature at the TFC in the experiment and analysis

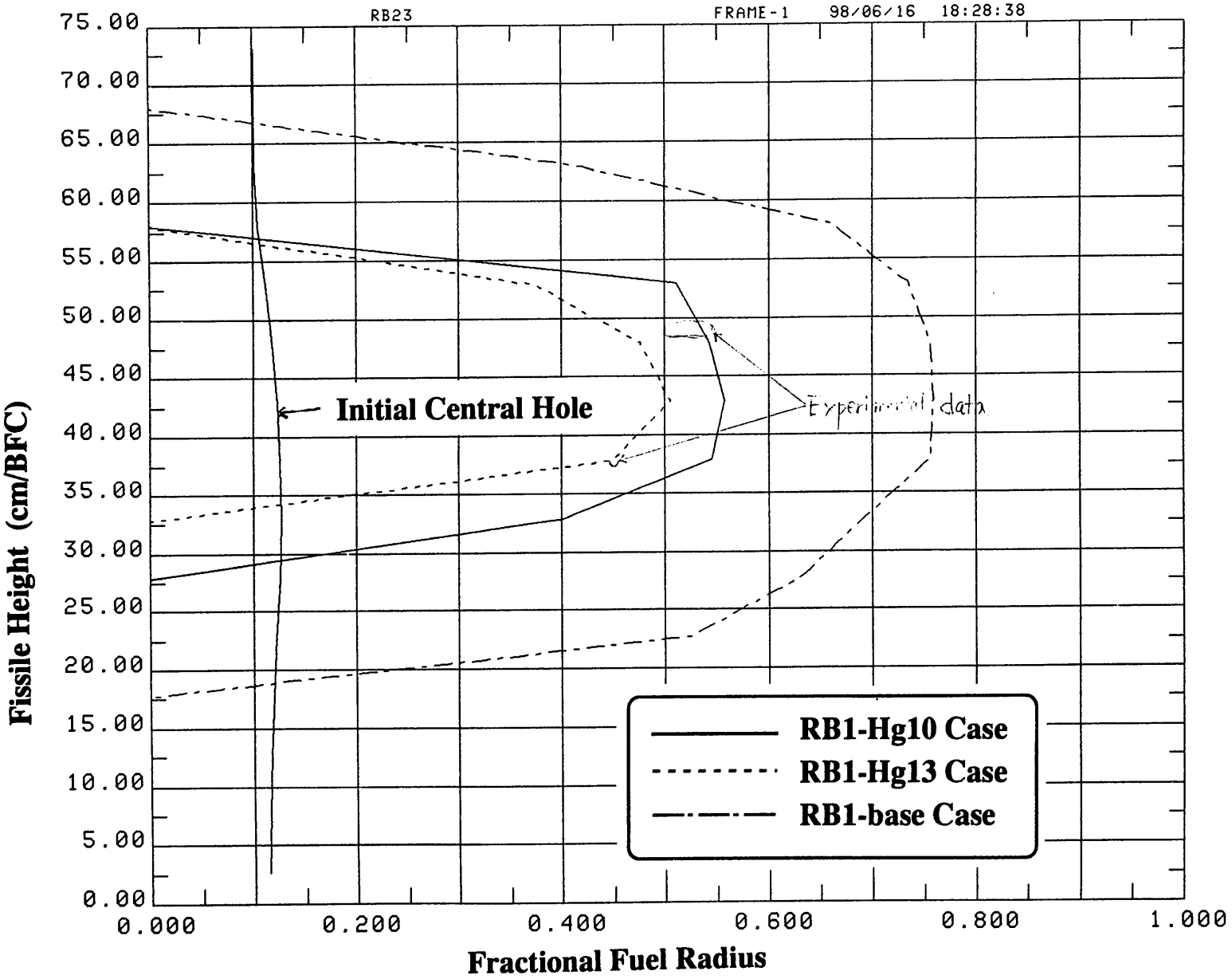

Fig. 3 Fuel melting boundaries just after the scram for each analysis case

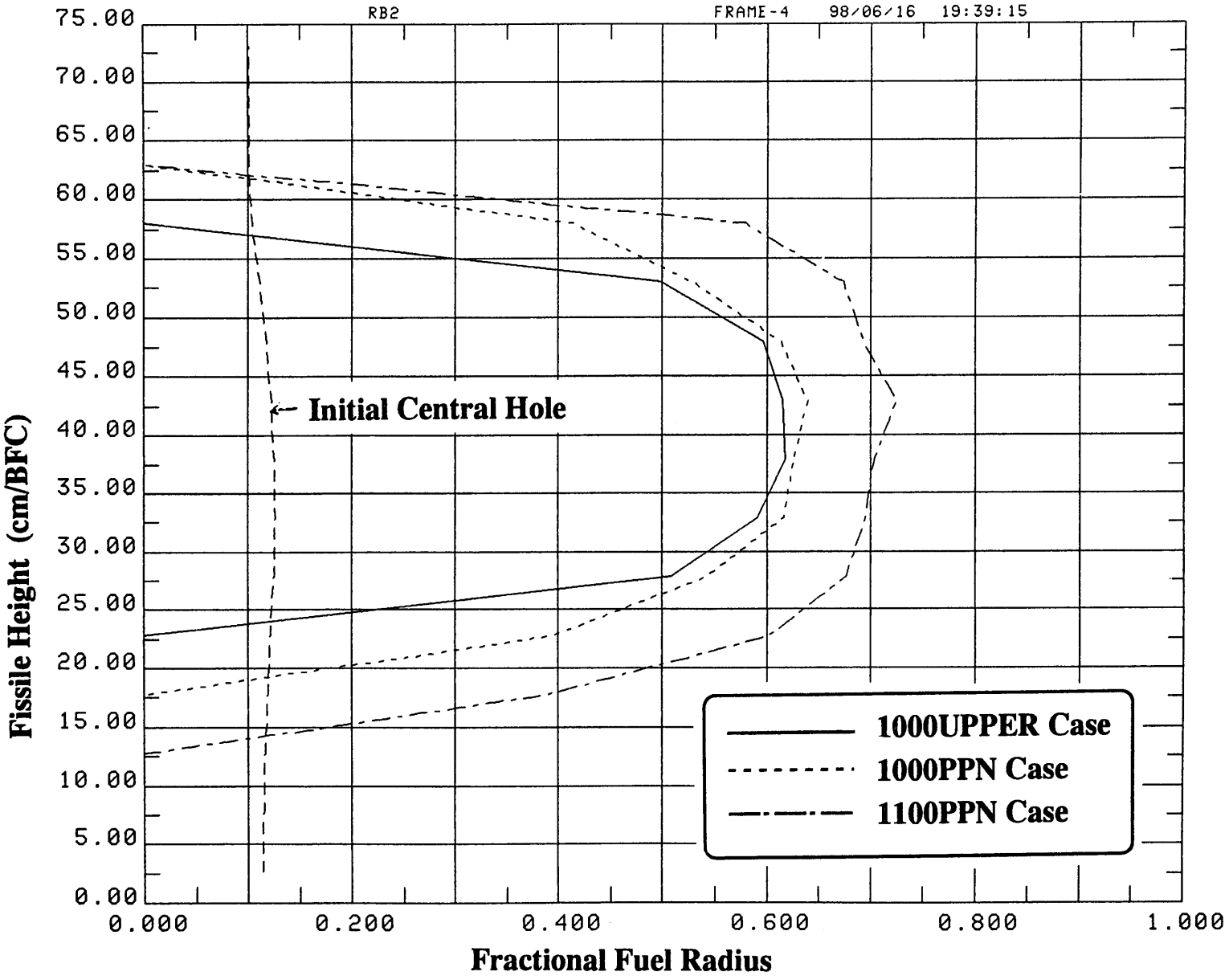

Fig. 4 Fuel melting boundaries just before the LOF onset for the 1000PPN, the 1100PPN and the 1000UPPER cases

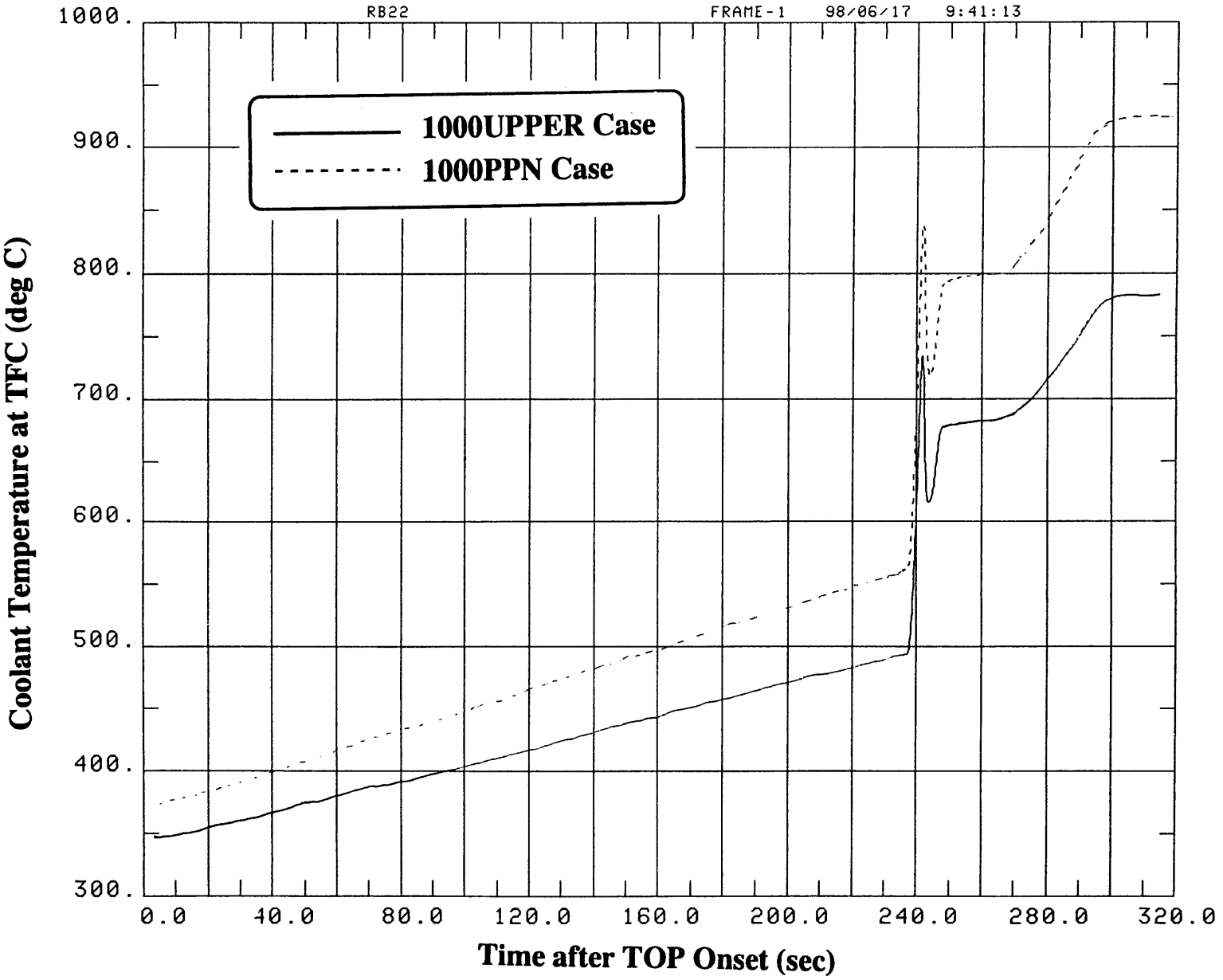

Fig. 5 Coolant temperature history at the TFC for the 1000PPN and the 1000UPPER cases

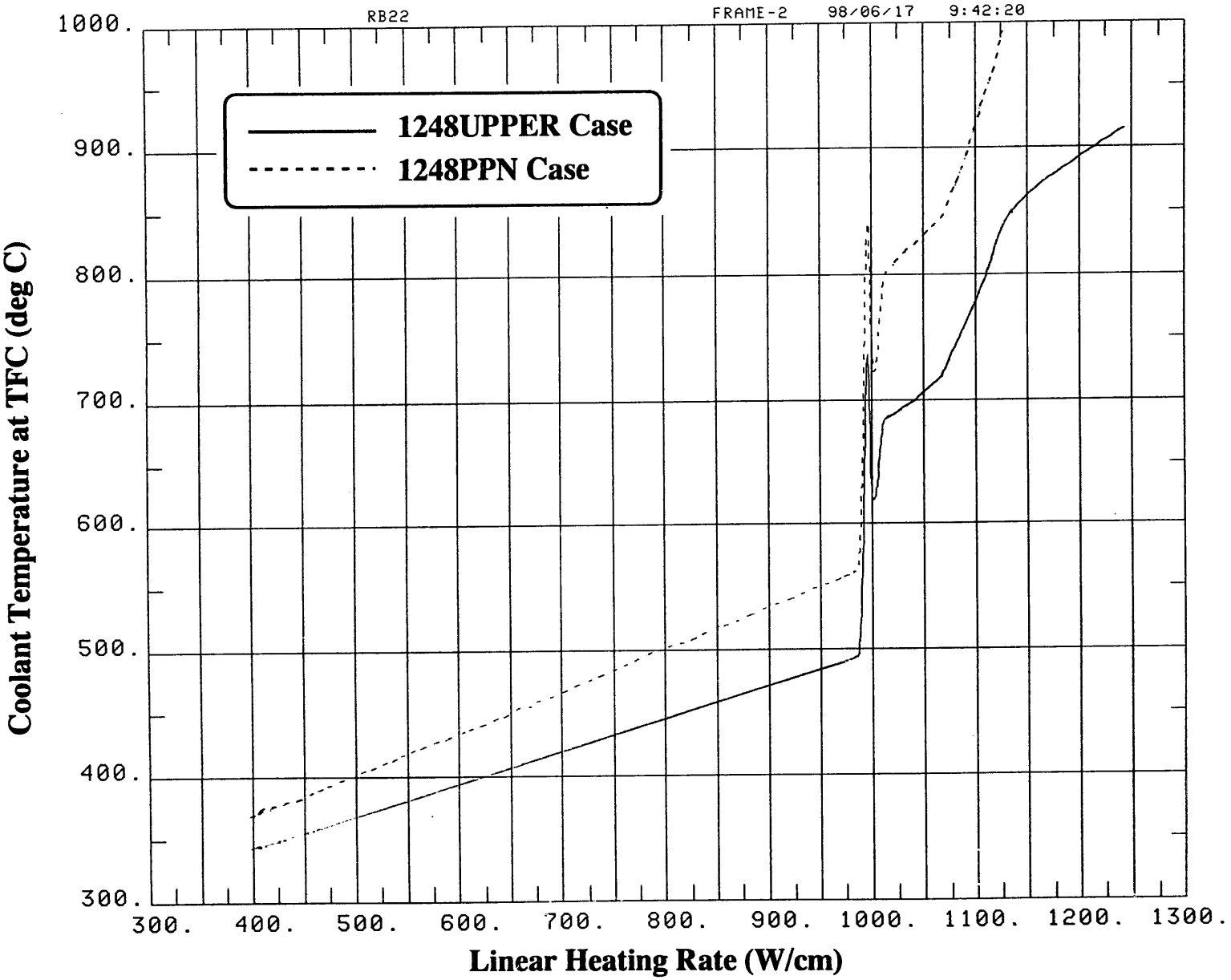

Fig. 6 Coolant temperature history at the TFC for the 1248PPN and the 1248UPPER cases

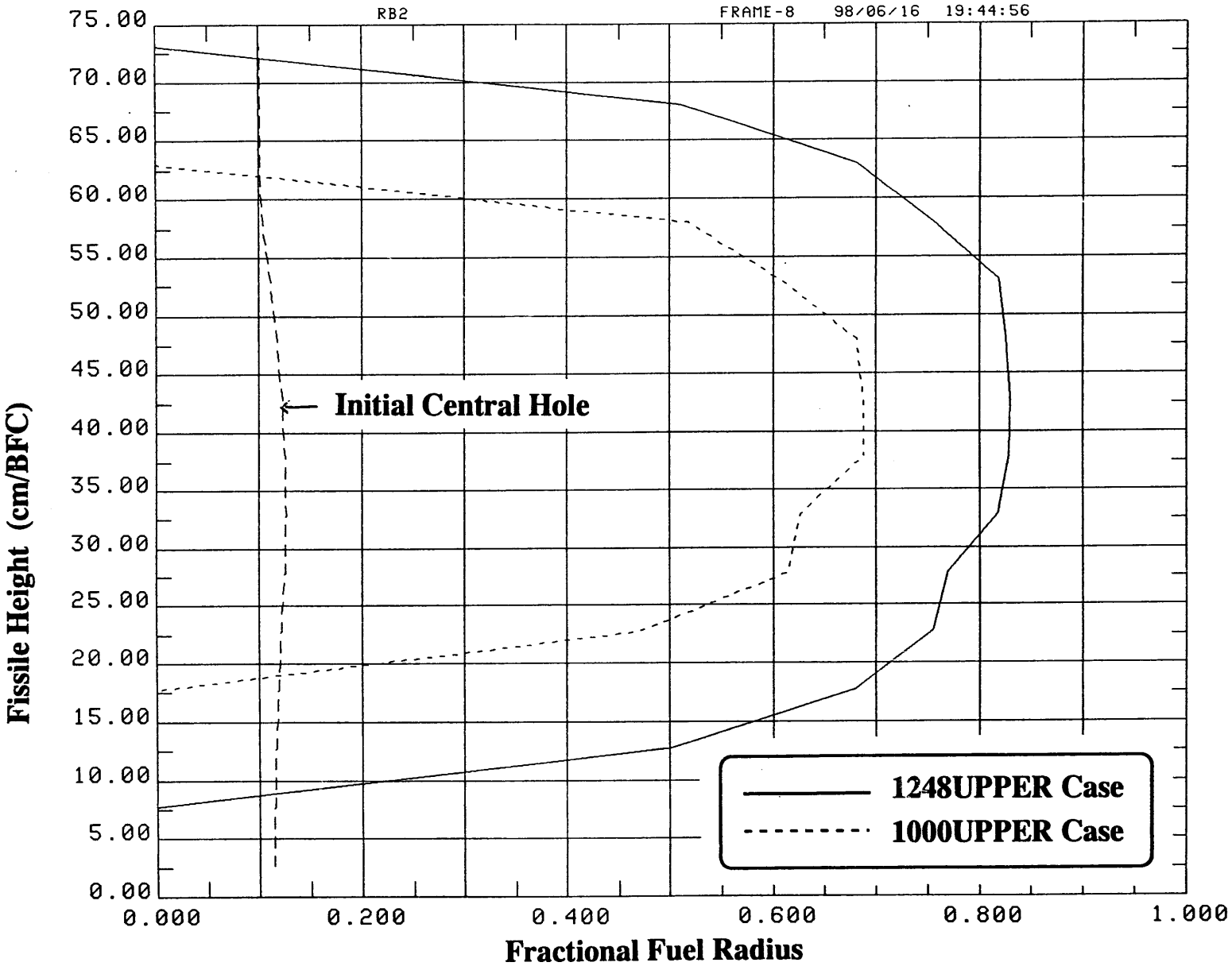

Fig. 7 Fuel melting boundaries just after the scram for the 1248UPPER and the 1000UPPER cases